

## Excited states of the proton emitter $^{105}\text{Sb}$

M. Lipoglavšek,<sup>1,2</sup> C. Baktash,<sup>1</sup> M. P. Carpenter,<sup>3</sup> D. J. Dean,<sup>1</sup> T. Engeland,<sup>4</sup> C. Fahlander,<sup>5</sup> M. Hjorth-Jensen,<sup>4</sup> R. V. F. Janssens,<sup>3</sup> A. Likar,<sup>2</sup> J. Nyberg,<sup>6</sup> E. Osnes,<sup>4</sup> S. D. Paul,<sup>1</sup> A. Piechaczek,<sup>7</sup> D. C. Radford,<sup>1</sup> D. Rudolph,<sup>5</sup> D. Seweryniak,<sup>3</sup> D. G. Sarantites,<sup>8</sup> M. Vencelj,<sup>2</sup> and C. H. Yu<sup>1</sup>

<sup>1</sup>Physics Division, Oak Ridge National Laboratory, Oak Ridge, Tennessee 37831

<sup>2</sup>J. Stefan Institute, Ljubljana, Slovenia

<sup>3</sup>Argonne National Laboratory, Argonne, Illinois 60439

<sup>4</sup>Department of Physics, University of Oslo, Oslo, Norway

<sup>5</sup>Department of Physics, Lund University, Lund, Sweden

<sup>6</sup>Department of Neutron Research, Uppsala University, Uppsala, Sweden

<sup>7</sup>Louisiana State University, Baton Rouge, Louisiana 70803

<sup>8</sup>Department of Chemistry, Washington University, St. Louis, Missouri 63130

(Received 25 February 2002; published 25 April 2002)

Excited states in the proton emitter  $^{105}\text{Sb}$  have been investigated for the first time. The nucleus was populated in the reaction  $^{50}\text{Cr}(^{58}\text{Ni},1p2n)$ . The GAMMASPHERE Ge-detector array was used together with Microball and the Neutron Shell for selection of the reaction channel. The experimental level scheme agrees well with results of a shell model calculation that uses realistic effective interactions derived from the CD-Bonn nucleon-nucleon interaction and  $^{100}\text{Sn}$  as a closed-shell core.

DOI: 10.1103/PhysRevC.65.051307

PACS number(s): 21.10.-k, 21.60.Cs, 23.20.Lv, 27.60.+j

Nuclei far from the line of  $\beta$  stability are at present in the focus of the nuclear structure physics community. Considerable attention has been devoted to nuclei close to the doubly-magic  $^{100}\text{Sn}$  nucleus and studies of proton-emitting nuclei, e.g., of systems beyond the drip line, have also started. All of these aspects are combined in the present paper which reports on the first observation of excited states in  $^{105}\text{Sb}$ , a nucleus which has four neutrons and one proton more than  $^{100}\text{Sn}$  and has been reported as a proton emitter [1].

The nucleus  $^{105}\text{Sb}$  was produced in the reaction  $^{50}\text{Cr}(^{58}\text{Ni},1p2n)$  at a beam energy of 225 MeV with a 2.1 mg/cm<sup>2</sup> thick target, enriched to more than 99% in  $^{50}\text{Cr}$ . The target was backed by 10 mg/cm<sup>2</sup> Au in order to stop the residual nuclei. The experiment was performed with the GAMMASPHERE Ge-detector array [2] at the ATLAS accelerator at Argonne National Laboratory. The experimental setup consisted of 78 Ge detectors, 95 CsI scintillators known as Microball [3] for light charged particle detection, and the newly developed Neutron Shell. The Neutron Shell consists of 30 liquid scintillator detectors for detection and identification of neutrons produced in fusion-evaporation reactions. The neutron detectors covered a solid angle of about  $1\pi$  in the forward direction from the target. The average detection and identification efficiencies for protons,  $\alpha$  particles, and neutrons were 78%, 47%, and 27%, respectively. The proton detection efficiency was found to depend somewhat on the proton energy and was slightly higher for reaction channels with lower particle multiplicity. The relatively low efficiency for  $\alpha$  particles is due to the thick target backing, thick absorbers in front of the detectors, and strict coincidence gating conditions; i.e., no  $\alpha$  particles could be identified in Microball detectors placed at angles  $\theta > 111.5^\circ$ . Due to the overlap of protons and  $\alpha$  particles in the backward detectors about 12% of  $\alpha$  particles were misinterpreted as protons. On the other hand, very few, only  $\sim 0.2\%$  of protons

were misinterpreted as  $\alpha$  particles. The separation between neutrons and  $\gamma$  rays detected in the neutron detectors was also very good: only 0.7% of the  $\gamma$  rays not connected with neutron emission were found in the spectra gated with one neutron. About 6% of the neutrons scattered from one detector into another and this could cause problems for identification of residual nuclei produced by the evaporation of two neutrons. However, the  $2n$  reaction channels could be identified by considering only events in which the two neutrons were not detected in neighboring neutron detectors. This technique, described in Ref. [4], reduced the neutron scattering probability to 3%, while the number of the real two neutron events decreased by 20%. This enabled us to clearly distinguish between  $2n$  and  $1n$  reaction channels. Further experimental details can be found in Ref. [5].

In the analysis, the data were sorted into particle gated  $\gamma$ -ray spectra and  $\gamma$ - $\gamma$  coincidence matrices. The detector setup provided very good reaction channel selection. Indeed, a total of 28 different residual nuclei were identified in 30 reaction channels, with the weakest being the  $2\alpha 2n$  channel leading to  $^{98}\text{Cd}$ .  $^{105}\text{Sb}$  was produced as a  $1p2n$  reaction. However, the  $1p2n$  gated  $\gamma$ -ray spectrum contained many  $\gamma$  rays from other reaction channels due to imperfect particle detection and identification. A weak 1219 keV  $\gamma$ -ray line was observed in the  $1p2n$  gated spectrum. It was not present in the corresponding  $2p2n$  nor in the  $1p1\alpha 2n$  gated spectra. In  $\gamma$ - $\gamma$  matrices, six  $\gamma$  rays were found to be in coincidence with this 1219 keV  $\gamma$  ray. Figure 1 presents the  $1p2n$  gated  $\gamma$ - $\gamma$  spectrum, and  $\gamma$  rays with energies 245, 287, 370, 495, 621, 735, 1079, and 1219 keV assigned to  $^{105}\text{Sb}$  are clearly visible.

Assuming that the particle detection efficiency is the same for reaction channels of similar particle multiplicity, the intensities of a specific  $\gamma$  ray in different particle gated spectra depend only on the multiplicity of each type of particle ac-

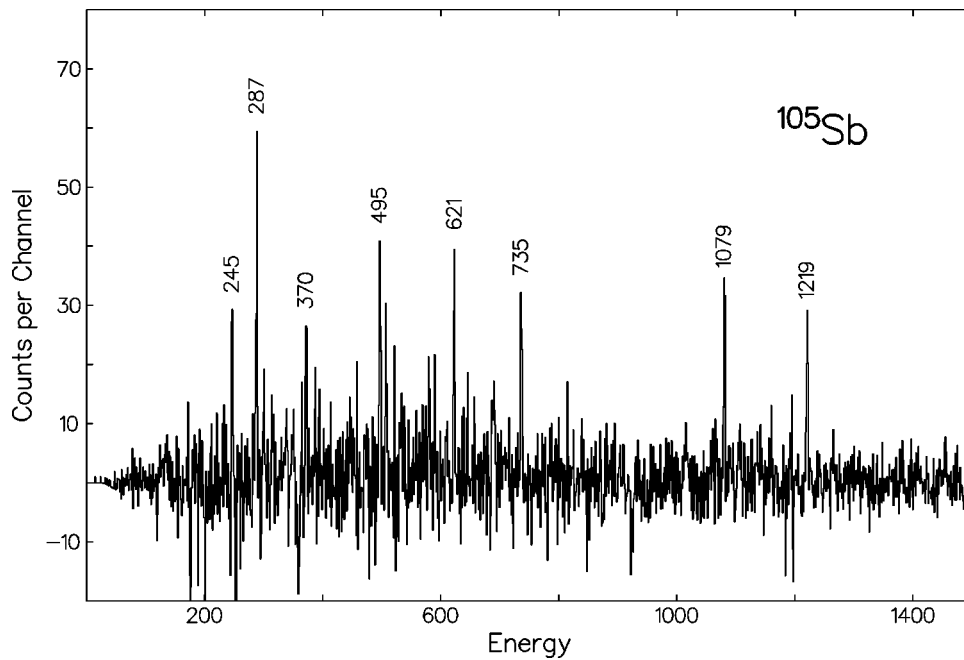


FIG. 1. Background subtracted  $1p2n$  gated  $\gamma$ - $\gamma$  coincidence spectrum. This spectrum only contains events for which the two neutrons were not detected in neighboring neutron detectors. The  $\gamma$ -ray gates were set on the 370, 621, and 1219 keV lines. The spectrum is a sum of the three gated spectra. The 1079 keV  $\gamma$  ray probably also belongs to  $^{105}\text{Sb}$ , but could not be placed in the level scheme due to a strong contamination from a transition with the same energy in  $^{105}\text{Sn}$ .

companying the electromagnetic emission. Thus, a comparison of the intensity ratios for a specific  $\gamma$  ray in two different particle gated spectra, with the intensity ratios for  $\gamma$  rays from previously known nuclei also observed in the experiment, enables an unambiguous assignment of the  $\gamma$  rays to the final nucleus. Results of such a comparison are shown in Fig. 2. Figure 2(a) gives the intensity ratio of the 370–1219 keV  $\gamma$ - $\gamma$  coincidence line as deduced from the matrices gated with two and one neutrons, respectively. It has a similar value as the intensity ratios of known lines belonging to  $^{104}\text{Sn}$  and  $^{101}\text{In}$  produced in reaction channels where two neutrons are emitted. Thus, the 370–1219 keV cascade does not belong to a one neutron channel that was observed in two neutron gated spectra due to neutron scattering between the detectors. Figure 2(b) shows again the intensity ratio of the 370–1219 keV  $\gamma$ - $\gamma$  coincidence line, but this time extracted from the matrices gated with one and zero protons. The measured ratio suggests that the 370–1219 keV cascade belongs to a  $1p$  channel. The 245, 287, 495, 621, and 735 keV  $\gamma$  rays also belong to the  $1p2n$  channel since they are in coincidence with both the 370 and 1219 keV lines. The above cascade could conceivably also be due to reactions on impurities in the target. The most abundant of these was a small amount of  $^{12}\text{C}$ , which was building up gradually during the experiment. To make sure that the  $\gamma$  rays are not due to unknown transitions in  $^{67}\text{As}$  populated in the reaction  $^{12}\text{C}(^{58}\text{Ni}, 1p2n)$ , we compared the  $\gamma$ -ray intensity from the beginning of the experiment, when the target was still fresh and contained little carbon, to the total intensity of a specific  $\gamma$  ray. The intensity ratio was 0.55 for the  $\gamma$  rays due to reactions on  $^{50}\text{Cr}$  and 0.29(7) for  $\gamma$  rays belonging to  $^{68}\text{As}$  as that were also seen in the experiment due to reactions on  $^{12}\text{C}$ . The corresponding ratio for the 370–1219 keV  $\gamma$ - $\gamma$  coincidence line was 0.57(13). No  $\gamma$  rays from reactions on

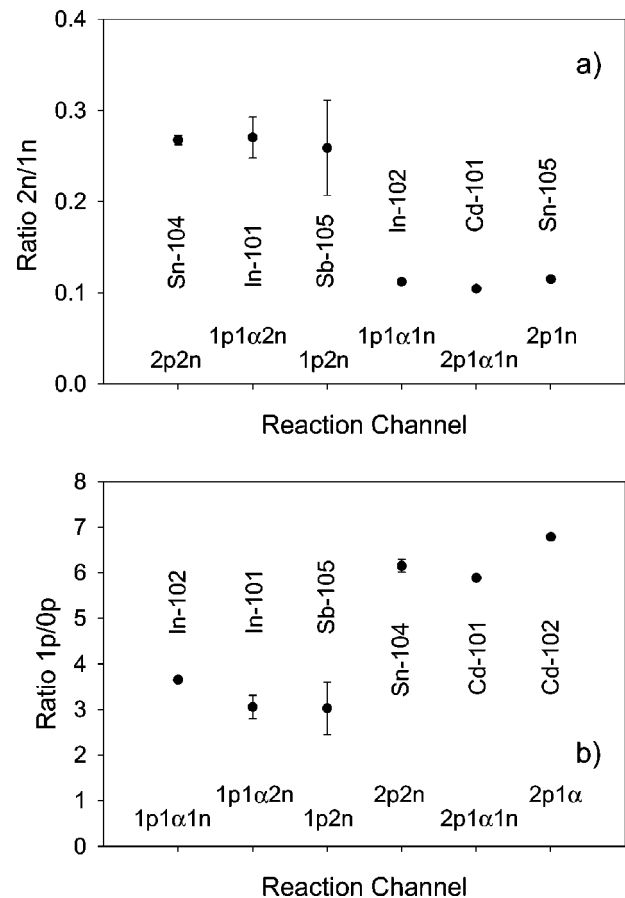


FIG. 2. Intensity ratios for different neutron (a) and proton (b) multiplicities. Differences in ratios for the same proton multiplicity in (b) are attributed to variance of the detection efficiency with respect to total particle multiplicity.

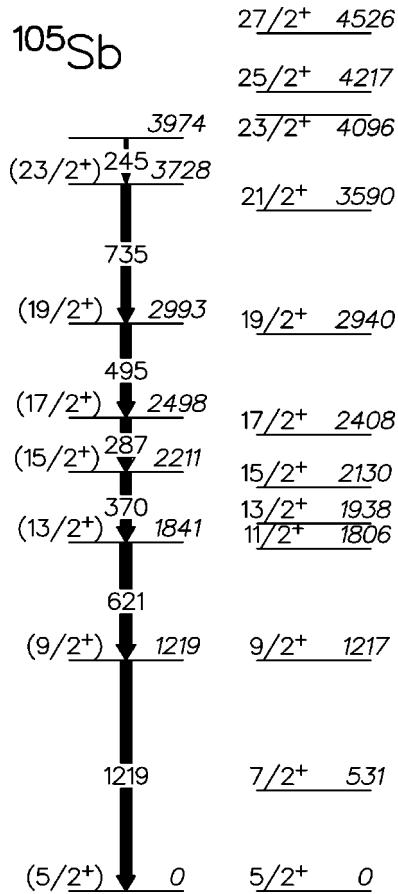


FIG. 3. Proposed level scheme for  $^{105}\text{Sb}$ . Shell model calculations are shown on the right-hand side. The widths of the arrows are proportional to the intensity of the transitions.

other target impurities were observed in the experiment. The above cascade is not known in nuclei that could possibly be populated by the evaporation of one proton and two neutrons from beam or target particles. We, therefore, conclude that the lines with energies 245, 287, 370, 495, 621, 735, and 1219 keV are due to transitions in  $^{105}\text{Sb}$ .  $^{105}\text{Sb}$  was populated in only 0.009% of the reactions. Assuming a calculated total reaction cross section of 330 mb this percentage translates into a 30  $\mu\text{b}$  cross section for the  $^{50}\text{Cr}(^{58}\text{Ni}, 1p2n)$  reaction.

The proposed level scheme is presented in Fig. 3. The first criterion for ordering the  $\gamma$  rays was their intensity, with the most intense ones at the bottom of the level scheme. However, we also relied on the systematics of heavier Sb isotopes, since many intensities are the same within  $1\sigma$  (see Table I). The multipolarities of the transitions were deduced by studying the  $\gamma$ -ray angular distributions. Intensity ratios as deduced from the summed spectrum of detectors at polar angles  $\theta=121.7, 129.9, 142.6, 148.3, \text{ and } 162.7^\circ$  vs detectors at  $\theta=69.8, 79.2, 80.7, 90.0, 99.3, 100.8, \text{ and } 110.2^\circ$  are given in Table I. The intensity ratios form two distinct groups with values around 0.6 and 1.3, respectively. We compared these ratios in  $^{105}\text{Sb}$  to similar ones for known transitions in other nuclei populated in the experiment. The first group of transitions corresponds to stretched dipole and the second to

TABLE I. Energies, intensities, and intensity ratios for  $\gamma$  rays belonging to  $^{105}\text{Sb}$ .

Energy (keV)	Relative intensity (a.u.)	Angular distribution intensity ratio	$J^\pi_{\text{initial}} \rightarrow J^\pi_{\text{final}}$
245.4(4)	5(2)		$\rightarrow (23/2^+)$
287.0(2)	18(3)	0.9(1)	$(17/2^+) \rightarrow (15/2^+)$
370.4(2)	18(3)	0.6(1)	$(15/2^+) \rightarrow (13/2^+)$
495.2(3)	17(4)	0.6(1)	$(19/2^+) \rightarrow (17/2^+)$
621.3(2)	20(4)	1.2(2)	$(13/2^+) \rightarrow (9/2^+)$
735.1(2)	16(4)	1.3(2)	$(23/2^+) \rightarrow (19/2^+)$
1079.4(5)			
1219.4(2)	19(7)	1.3(1)	$(9/2^+) \rightarrow (5/2^+)$

stretched quadrupole transitions. Mixed  $E2/M1$  transitions correspond to ratios with values intermediate between 0.6 and 1.3. The level scheme of  $^{105}\text{Sb}$  shown in Fig. 3 was constructed assuming that only stretched  $M1$ ,  $E2$  and mixed  $E2/M1$  transitions were observed and that the spins of the levels increase with excitation energy. The observed ground state proton decay of  $^{105}\text{Sb}$  was best explained by assuming  $J^\pi=5/2^+$  for the ground state [1]. Therefore, these quantum numbers are adopted here. Nevertheless, since the spin and parity of the ground state have not been measured directly, all our spin and parity assignments are considered to be tentative.

The high spin level scheme of  $^{105}\text{Sb}$  resembles that of  $^{107}\text{Sb}$  up to  $J=19/2$  [6]. In fact, the comparison between the  $^{107}\text{Sb}$  and  $^{105}\text{Sb}$  level schemes mirrors the one that can be made for the  $^{106}\text{Sn}$  to  $^{104}\text{Sn}$  nuclei. This implies that coupling a  $d_{5/2}$  proton to a  $^{104}\text{Sn}$  core is appropriate to describe the observed states, and is confirmed by the shell model calculation displayed on the right-hand side of Fig. 3. The calculation uses  $^{100}\text{Sn}$  as closed shell core with effective interactions for the four valence neutrons and one valence proton based on the CD-Bonn nucleon-nucleon interaction [7]. These effective two-body interactions are in turn used in a shell-model calculation for valence neutrons and protons in the single-particle orbits  $2s_{1/2}$ ,  $1d_{5/2}$ ,  $1d_{3/2}$ ,  $0g_{7/2}$ , and  $0h_{11/2}$ . More details about effective interactions for nuclei near  $A \sim 100$  can be found in Ref. [8]. Such effective interactions were used recently to describe the newly observed spectrum of  $^{106}\text{Sb}$  [9].

The calculation favors a  $J^\pi=5/2^+$  assignment for the ground state, in agreement with the suggestion from the proton decay data. In this state, the valence proton occupies mainly the  $d_{5/2}$  orbit and the two neutron pairs are almost evenly distributed over the  $d_{5/2}$  and  $g_{7/2}$  orbits. The situation is very similar in the  $9/2^+$  and  $13/2^+$  levels, while the  $\nu d_{5/2}^3 g_{7/2}^1$  configuration exhausts the largest components of the wave functions of the  $15/2^+$  and  $17/2^+$  states. The neutron part of the wave function of the  $19/2^+$  level is almost identical to that of the  $17/2^+$  state. However, since  $17/2$  is the maximum spin for the  $\pi d_{5/2}^1 \nu d_{5/2}^1 g_{7/2}^1$  configuration with the remaining neutron pair coupled to  $J=0$ , the odd proton resides almost exclusively in the  $g_{7/2}$  orbit in the  $19/2^+$  state. This  $19/2^+$  level is, therefore, the lowest lying of the ob-

served states, in which the  $\pi g_{7/2}$  orbit has a significant contribution to the wave function. This pattern repeats itself for the states with spins  $21/2^+$ ,  $23/2^+$ ,  $25/2^+$ , and  $27/2^+$  in an alternating fashion, with the state  $21/2^+$  having a proton in the single-particle orbit  $\pi d_{5/2}$ . For proton degrees of freedom, the  $s_{1/2}$ ,  $d_{3/2}$ , and  $h_{11/2}$  single-particle orbits give essentially negligible contributions to the wave functions and energies of the excited states. For neutrons, although the single-particle distribution for a given state is also negligible, these orbits are important for a good description of the energy spectrum, as was also demonstrated in large-scale shell-model calculations of the tin isotopes [10]. The effective interaction employed here is the same as that used in Ref. [10]. In general, it provides a satisfactory reproduction of the data.

It is worth noting that the agreement with the experimentally proposed spin assignment is very good. The reason for such an agreement is most likely that the wave functions of the states are dominated by neutron degrees of freedom. The unbound proton is only a spectator, while the well-bound neutrons change orbits and alignment in transitions from high spin states to the ground state.

The recently described spectrum of  $^{107}\text{Sb}$  also exhibits low-lying  $7/2^+$  and  $11/2^+$  states, located at approximately the same excitation energies as those computed in the theoretical calculation discussed here. The  $\gamma$ -ray transitions feeding these two states in  $^{105}\text{Sb}$  are, as in  $^{107}\text{Sb}$ , expected to be

much weaker than the main  $\gamma$ -ray cascade. This presumably explains why these two states were not identified in the experiment. They are nevertheless interesting since their wave functions contain mainly contributions from the  $\pi g_{7/2}$  orbit that is poorly known near  $^{100}\text{Sn}$ . A more sensitive experiment is clearly needed for their identification.

In conclusion, we have for the first time identified excited states in  $^{105}\text{Sb}$ , a nucleus located beyond the proton drip line. Despite the unbound proton,  $\gamma$ -ray decay along the yrast line remains the primary mode of decay from high-spin states. The experimental level scheme agrees very well with shell model calculations.  $^{105}\text{Sb}$  is now the lightest ground state proton emitter and the lightest Sb isotope with known excited states. The combination of GAMMASPHERE, Microball, and the Neutron Shell proved to constitute an excellent detector setup for identifying weakly populated reaction channels in fusion evaporation reactions.

Oak Ridge National Laboratory is operated by UT-Battelle, LLC for the U.S. Department of Energy under Contract No. DE-AC05-00OR22725. Work at Argonne National Laboratory was supported by the U.S. Department of Energy under Contract No. W-31-109-ENG-38 and at Washington University under Contract No. DE-FG02-88ER40406.

- 
- [1] R.J. Tighe, D.M. Moltz, J.C. Batchelder, T.J. Ognibene, M.W. Rowe, and J. Cerny, *Phys. Rev. C* **49**, R2871 (1994).
  - [2] I.Y. Lee, *Nucl. Phys.* **A520**, 361 (1990).
  - [3] D.G. Sarantites *et al.*, *Nucl. Instrum. Methods Phys. Res. A* **381**, 418 (1996).
  - [4] J. Cederkäll *et al.*, *Phys. Rev. C* **53**, 1955 (1996).
  - [5] M. Lipoglavšek *et al.*, *Proceeding of the International Conference on Nuclear Structure 2000* [*Nucl. Phys.* **A682**, 399c (2001)].
  - [6] D.R. LaFosse *et al.*, *Phys. Rev. C* **62**, 014305 (2000).
  - [7] R. Machleidt, F. Sammarruca, and Y. Song, *Phys. Rev. C* **53**, R1483 (1996).
  - [8] M. Hjorth-Jensen, T.T.S. Kuo, and E. Osnes, *Phys. Rep.* **261**, 125 (1995); T. Engeland, M. Hjorth-Jensen, and E. Osnes, *Phys. Rev. C* **61**, 021302(R) (2000).
  - [9] D. Sohler, *et al.*, *Phys. Rev. C* **59**, 1324 (1999).
  - [10] A. Holt, T. Engeland, M. Hjorth-Jensen, and E. Osnes, *Nucl. Phys.* **A634**, 41 (1998).